JOURNAL OF VIROLOGY, July 1972, p. 99-114
Vol. 10, No. 1

Printed in U.S.A.

Direction of Translation and Size of Bacteriophage φX174 Cistrons

ROBERT M. BENBOW, ROBERT F. MAYOL, JOANNA C. PICCHI, AND ROBERT L. SINSHEIMER

Division of Biology, California Institute of Technology, Pasadena, California 91109

Received for publication 20 March 1972

Translation of the bacteriophage φX174 genome follows cistron order D-E-F-G-H-A-B-C. To establish this, the position of a nonsense mutation on the genetic map was compared with the physical size (molecular weight) of the appropriate protein fragment generated in nonpermissive cells. Distances on the φX174 genetic map and distances on a physical map constructed from the molecular weights of φX174 proteins and protein fragments are proportional over most of the genome with the exception of the high recombination region within cistron A.

Nonsense mutations—amber (UAG), ochre (UAA), or opal (UGA)—are found in nine cistrons of bacteriophage φX174 (1, 9). Translation of a cistron containing one of these altered codons under nonpermissive conditions causes premature termination of a φX174-specific protein (3, 6, 7, 11). The size of the protein fragment generated should depend on the location of the mutation relative to the N-terminal coding end of the cistron. Thus, by assuming a direction of transcription and translation, the genetic map of φX174 (1) may be used to predict the effect of a nonsense mutation in a given cistron on the size of the polypeptide chain specified by that cistron. Furthermore, since the genome of φX174 is transcribed from the complementary strand (8) as a polycistronic message (9), strong polar mutations may exist at the initiator (N-terminal) end of some cistrons (19).

Sodium dodecyl sulfate (SDS) polyacrylamide gel electrophoresis was employed to separate φX174-specific proteins and polypeptide fragments on the basis of size (14). The gel patterns obtained after infection with several φX174 nonsense mutants in a single cistron were then compared with the map order of these mutations established by three-factor genetic crosses. In this way, the direction of translation of each of several cistrons has been established independently. Furthermore, several strong polar mutations were found that eliminate two or more φX174-specific proteins from the gel patterns. Using this information, it is found that all φX174 cistrons examined are translated in the same direction. This direction is identical to that previously established for the related bacteriophage S13 by the Tessman group (15, 17).

Distances on the genetic map (i.e., recombination frequencies obtained in two-factor genetic crosses) were compared with the physical size (molecular weight) of each full or partial cistron product. The genetic and physical maps are colinear over the entire genome. In addition, genetic and physical distances are reasonably proportional except in the high recombination region of cistron A. This proportionality implies that physical distances (for example, φX174 RF deoxyribonucleic acid [DNA] contour lengths measured in the electron microscope) may subsequently be used to define the relative location on the genetic map of structural features such as the φX174 cistron E deletion (A. J. Zuccarelli, R. M. Benbow, and R. L. Sinsheimer, Proc. Nat. Acad. Sci. U.S.A., *in press*).

MATERIALS AND METHODS

Bacteriophage stocks. Bacteriophage φX174 nonsense mutants, growth procedures, and methods for three-factor genetic crosses were described previously (1). *Escherichia coli* C and HF4701 (7) are nonpermissive strains for all nonsense mutants used in this study.

Media. TPG (10) consisted of NaCl, 0.05 g; KCl, 8.0 g; NH_4Cl, 1.1 g; $MgCl_2$, 0.2 g; tris(hydroxymethyl)aminomethane (Tris), 12.1 g; KH_2PO_4, 0.023 g; sodium pyruvate, 0.8 g; and 0.16 M Na_2SO_4, 1 ml. Distilled water was added to make 1 liter, and 1.0 ml of sterile 1 M $CaCl_2$ and 10 ml 20% glucose were added after autoclaving.

Lysis buffer (7) contained sucrose, 120 g; Tris, 6 g (adjust to *p*H 8.0 in small volume of distilled water); SDS, 10 g; 2-mercaptoethanol, 10 g; sodium azide, 0.65 g. Distilled water was added to buffer to make 1 liter. This solution should not be autoclaved.

Five percent sucrose contained sucrose, 50 g; NaCl, 29.2 g; Tris, 6.0 g; and EDTA (disodium dihydrogen

ethylenediaminetetraacetate dihydrate), 1.86 g. The *p*H was adjusted to 8.0 with HCl and distilled water added to make 1 liter. This solution should not be autoclaved.

Twenty percent sucrose contained sucrose, 200 g; NaCl, 29.2 g; Tris, 6.0 g; and EDTA, 1.86 g. The *p*H was adjusted to 8.0 with HCl and distilled water added to make 1 liter. This solution should not be autoclaved.

Molecular-weight standards. Cytochrome *c*, myoglobin, chymotrypsinogen A, ovalbumin, and albumin were obtained as molecular-weight marker kit 20900-8109 from Mann Research Laboratories.

^{3}H-labeled ribonuclease was obtained from Worthington Biochemical Corp.

Reagents. Diethyl pyrocarbonate was obtained from Eastman Kodak Corporation. NCS solubilizer was obtained from Amersham/Searle. Liquifluor was obtained from New England Nuclear Corp.

Preparation of φX174-specific proteins in unirradiated cells. This double-label procedure is described in detail in Mayol and Sinsheimer (11) and is used only when gel patterns are calculated from the distribution of radioactive proteins in gel slices.

E. coli C was grown in TPG (supplemented with 10 μg of adenine per ml) at 37 C with aeration to a concentration of 3×10^8 cells per ml. φX174 *wt* or nonsense mutant phage was added at multiplicity of infection (MOI) of 3. Fifteen minutes after infection, 5 μCi of ^{14}C-leucine (311 mCi/mmole, Schwarz BioResearch, Inc.) was added to each 5-ml culture; 5 min later the culture was chilled to 0 C and centrifuged, and the pellet was resuspended in 0.2 ml 0.05 M Tris (*p*H 8.0). A 0.1-ml amount of lysozyme (2 mg/ml) and 0.1 ml of 0.01 M EDTA were added, and the mixture was incubated for 10 min at 37 C. After freeze-thawing the cells three times to insure lysis, 0.1 ml of 1 mg of deoxyribonuclease per ml in 1 M $MgSO_4$ was added. The lysate was dialyzed overnight at 4 C against 0.05 M Tris (*p*H 8.0).

Uninfected cells were labeled with 100 μCi of ^{3}H-leucine (2 Ci/mmole, Schwarz BioResearch, Inc.) per 5 ml of culture and treated identically.

To make higher activity extracts, 25 ml of infected labeled cells were lysed in the same volume used above for 5 ml.

To denature the proteins prior to electrophoresis, 25 μliters of ^{3}H-labeled uninfected lysate and 25 μliters of ^{14}C-labeled infected lysate were mixed with 58.5 mg of urea, 5 μliters of 10% 2-mercaptoethanol, and 12 μliters of 1% SDS. This mixture was incubated for 3 hr at 37 C and then immersed in boiling water for 10 min prior to electrophoresis.

Preparation of ^{14}C-labeled φX174-specific proteins for autoradiography. This procedure is described in detail by Godson (7). We thank G. N. Godson for instruction in his laboratories at the Yale University School of Medicine.

E. coli HF4701 was grown in TPG at 37 C with aeration to 2.5×10^8 cells/ml. Thirty milliliters were removed to a 100-mm circular plastic petri dish and ultraviolet (UV)-irradiated for 5 min at 19 ergs per mm^2 per sec. The irradiated cells were aerated for 10 min and then 2.5-ml samples were added to growth tubes containing 3 μCi of ^{14}C-leucine and 6.3×10^9 phage (MOI = 10). After 35 min at 37 C with aeration, the infected cells were pelleted (6,000 rev/min for 20 min), and stored frozen until use.

Lysis buffer (200 μliters) was used to resuspend the thawed pellet. The tubes were placed in boiling water for 10 min (to insure complete denaturation) prior to electrophoresis.

Preparation of ^{14}C- or ^{3}H-labeled φX174 virions. *E. coli* C, a nonpermissive host for *am* mutations, was grown in TPG at 37 C with aeration to a concentration of 3×10^8 cells/ml. The culture was infected at a MOI of 3 with φX174 *wt* or with a φX174 nonsense (*am*) mutant. ^{3}H-leucine (20 μCi/ml) or ^{14}C-leucine (1 μCi/ml) was added 7 min after infection. Under these conditions *am* mutations in most cistrons prevent the formation of complete φX174 virions. However, cistron E mutants (the "lysis" cistron) produce very large numbers of infective intracellular phage. In addition, cistron H mutants (*am*N1, *am*23, *am*80, and *op*11) and *am*6 in cistron J? package infective single-stranded DNA into noninfective virions which are unable to infect or to lyse the host cells. We shall call these virions defective particles.

After 45 min at 37 C, cistron E, J?, and H cell-phage complexes were pelleted (6,000 rev/min for 20 min) and lysed with 0.4 ml of 0.05 M Tris, 0.005 M EDTA, and 0.2 mg of lysozyme (*p*H 8.0) per ml. Lysates were banded twice in CsCl ($\rho \cong 1.40$) for 36 hr in a Spinco SW50.1 rotor at 50,000 rev/min and then were sedimented through a 5 to 20% sucrose gradient in a Spinco SW25.1 rotor for 4 hr at 22,000 rev/min. Pooled fractions containing the defective particles were dialyzed at 4 C overnight against two changes of 0.05 M Tris, *p*H 8.0.

An appropriate volume (usually 100 μliters) was mixed with 100 μliters of lysis buffer and then was immersed in boiling water for 10 min prior to electrophoresis.

Preparation of SDS polyacrylamide gels. Gels for double-label analysis were run in Pyrex glass tubes (7 by 75 mm); gels for autoradiography and for molecular-weight standardizations were run in glass tubes (9 by 75 mm).

Fifteen percent polyacrylamide gels were prepared (11) by mixing 2.0 ml of 60% acrylamide-0.5% bis-acrylamide, 1.0 ml of solution A, 0.8 ml of 1% SDS, 0.2 ml of distilled water, and 5 μliters of Temed. Solution A contained 48 ml of 1 N HCl, 36.6 g of Tris (*p*H 8.9), 0.23 ml of Temed, and distilled water to make to 100 ml. A 4-ml amount of fresh ammonium persulfate solution containing 0.14 g per 100 ml of solution was added to catalyze polymerization. After mixing, the solution was rapidly transferred to the Pyrex glass tubes. Water was gently layered over each gel to smooth the upper interface.

Ten percent gels contained 1.0 ml of solution A, 0.8 ml of 1% SDS, 1.33 ml of 60% acrylamide-0.5% bis-acrylamide, 5 μliters of Temed, and 0.87 ml of distilled water. A 4.0-ml amount of fresh ammonium persulfate solution containing 0.14 g per 100 ml of solution was added to catalyze polymerization.

Twenty percent gels contained 1 ml of solution A, 0.8 ml of 1% SDS, 2.6 ml of 60% acrylamide-0.5% bis-acrylamide, and 5 μliters of Temed. A 3.54-ml amount of fresh ammonium persulfate solution con-

taining 0.14 g per 100 ml of solution was added to catalyze polymerization.

Polyacrylamide gel electrophoresis. Gels were prerun in gel buffer (0.375 M Tris, *p*H 8.9, 0.1% SDS) for 45 min at 4 ma/gel. The gel buffer was removed from the electrophoresis apparatus and replaced with running buffer. Running buffer contained 1 g of SDS, 2.88 g of glycine, 0.6 g of Tris (*p*H 8.3) per liter. The denatured proteins (plus bromphenol blue dye marker) were layered onto the top of the gel. Electrophoresis was begun at 2 ma/gel for 20 min to "stack," and then the current was increased to 4 ma/gel for about 2.5 hr.

Measurement of radioactive φX174-specific proteins. Frozen double-label gels were usually sectioned by using a device having a series of razor blades at 1-mm intervals. As this work was being completed, we were introduced to the Mickel Gel Slicer (Brinkman Instruments, Westbury, N. Y.). This instrument unquestionably produces more uniform, reproducible slices. Slices were extracted in 5 ml of scintillation fluid for 12 hr and then counted in a Beckman liquid scintillation counter. Scintillation fluid contains 90 ml of NCS solubilizer, 10 ml of water, 42 ml of Liquifluor, and 858 ml of toluene per liter of solution.

φX-specific $\Delta^{14}C$ counts were calculated from the $^{14}C/^{3}H$ ratios as described by Mayol and Sinsheimer (11).

Gels for autoradiography were frozen overnight in 10% acetic acid, unthawed, sliced longitudinally, and dried under vacuum on filter paper. Exposures were generally for 2 days with Kodak no-screen X-ray film.

Molecular-weight standardization. To determine the molecular weight of each φX174-specific protein, 10 μg of a protein of known molecular weight was run in the same gel with ^{3}H- or ^{14}C-labeled φX174 proteins. Cytochrome *c* (12,400), myoglobin (17,800), chymotrypsinogen A (25,000), ovalbumin (45,000), and albumin (67,000) were used as markers. The gel was stained for 10 hr in 0.25% Coomassie Brilliant Blue (dissolved in 5:5:1 solution of methanol-water-acetic acid) and then was destained for 36 hr in a 5:5:1 solution of methanol-water-acetic acid. The concentrations of the radioactive proteins were low enough that they were not visibly stained. The gel was sectioned into 1-mm slices and each slice was counted in scintillation fluid. RF values for each marker protein were calculated from the position of furthest migration of a bromphenol blue marker. Gels were normalized so that cistron D protein ran with an $RF_{15\%} = 0.725$.

Similar standardization was carried out with diethyl pyrocarbonate-treated ^{3}H-labeled ribonuclease (13,700) run in the same gel with ^{14}C-labeled φX174-specific proteins. Treatment with diethyl pyrocarbonate causes the formation of ribonuclease dimers (~27,400), trimers (~41,100), and tetramers (~54,800) (18).

RESULTS

Thirteen proteins are observed in greater amounts in φX174-infected cells than in uninfected cells. Two of these apparently are host-coded proteins since they are not observed under conditions where the host cells are heavily UV-irradiated prior to infection. A third protein of high molecular weight may also represent, in part, a host-coded protein. It is seen, however, in UV-irradiated cells. The other 10 proteins presumably are coded for by the φX174 genome.

(i) φX174 wt proteins. The distribution of ^{14}C-labeled φX174-specific proteins made in UV-irradiated cells is shown after electrophoresis on 15% polyacrylamide SDS gels in the autoradiograph of Fig. 1a. Clearly visible bands are seen at

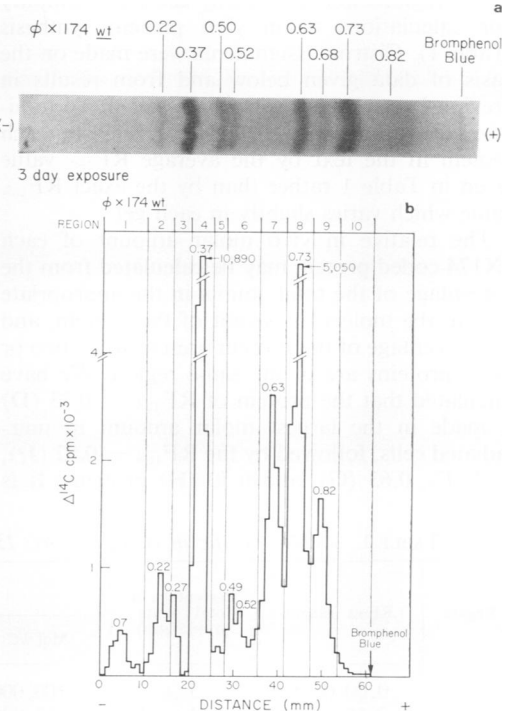

FIG. 1. *(a) An autoradiograph of a 15% polyacrylamide SDS gel of a lysate of ^{14}C-labeled wt-infected UV-irradiated cells. The average mobility (i.e., the $RF_{15\%}$ taken from Table 1) of each clearly visible band relative to a bromphenol blue marker is indicated; this does not correspond necessarily to the exact mobility visible in the autoradiograph because of shrinkage and distortion during the slicing and drying procedure. (b) A 15% polyacrylamide SDS gel electrophoresis pattern of an extract of a lysate of ^{14}C-labeled wt-infected cells mixed with an extract of a lysate of ^{3}H-labeled uninfected cells. Phage φX174-specific ($\Delta^{14}C$) counts are plotted versus migration distance (millimeters) from the origin. The exact (not average) mobility of each distinct peak relative to a bromphenol blue marker is indicated. Ten arbitrary regions (see Table 1) are indicated at the top of the figure to simplify calculations. Each region was eluted, treated with 9 M urea, 0.1% SDS for 3 hr at 37 C, immersed in boiling water for 10 min, and rerun on 10% gels. Over 90% of the proteins in each region were stable to this treatment, running as a compact region on the lower percentage gels.*

$RF_{15\%}$ values (relative to a bromphenol blue dye marker) of 0.22, 0.37, 0.50, 0.52, 0.63, 0.68, 0.73, and 0.82. Bands which are not clearly visible may exist at 0.59, 0.75, and 0.84.

The distribution of ^{14}C-labeled ϕX174-specific proteins made in unirradiated cells and detected by a double-label analysis is shown in Fig. 1b after electrophoresis on 15% polyacrylamide SDS gels. $\Delta^{14}C$ counts are plotted versus distance of migration by using the procedure of Mayol and Sinsheimer (11).

Ten regions were arbitrarily chosen to simplify our calculations of in vivo protein synthesis (Table 1). Cistron assignments were made on the basis of data given below and from results in previously published work (3, 6, 7, 11). To minimize confusion, we shall always refer to each protein in the text by the average $RF_{15\%}$ value given in Table 1 rather than by the exact $RF_{15\%}$ value which varies slightly in each gel.

The relative in vivo molar amount of each ϕX174-coded protein may be calculated from the percentage of the total counts in the appropriate region, the molecular weight of the protein, and the percentage of the protein present when two or more proteins are in the same region. We have calculated that the protein of $RF_{15\%}$ = 0.73 (D) is made in the largest molar amount in unirradiated cells, followed by the $RF_{15\%}$ = 0.82 (J?), 0.37 (F), 0.63 (G), and 0.50 (H) proteins. It is difficult to make a quantitative estimate for the $RF_{15\%}$ = 0.68 (E) protein (no clear peak) or for any of the other ϕX174-specific proteins which appear to be made in smaller molar amounts.

(ii) Molecular weights of ϕX174-specific proteins. Two procedures were used to estimate the molecular weight of ϕX174 proteins and polypeptide fragments: comparison in the same gel with unlabeled proteins of known molecular weight identified by staining, and comparison in the same gel with ^3H-labeled ribonuclease monomers, dimers, trimers, and tetramers. A composite calibration curve for 15% gels is shown in Fig. 2. The molecular weights (Table 1) of the 10 putative ϕX174-coded proteins sum to 228,000 daltons, roughly the entire capacity of the ϕX174 genome [1,833 codons × 124 (estimated from the average amino acid composition of ϕX174 coat proteins [reference 4 and *unpublished data*]) molecular weight/average amino acid ≅227,000 daltons)]. If the $RF_{15\%}$ = 0.22 (67,000 molecular weight) protein is entirely coded for by the ϕX174 genome as implied by Godson (7), then several of these proteins must represent other than single ϕX174 cistron products.

(iii) Order of ϕX174 cistrons and of nonsense mutations within cistrons. The genetic map of bacteriophage ϕX174 has nine cistrons of order D-E-F-G-H-A-B-C-I (1, 9). The exact position of I is uncertain; a tenth (tentative) cistron, J,

TABLE 1. *ϕX174-specific in vivo proteins: 15% sodium dodecyl sulfate polyacrylamide gels*

Region	$RF_{15\%}$ (range)	Percentage of total counts (n = 5 gels)	Cistron assignments		
			Mol wt	$RF_{15\%}$	Cistron
1	0.00–0.15	5 ± 3	~100,000	0.05 ± 0.02[a]	Host
2	0.15–0.25	4 ± 1	67,000	0.22 ± 0.03	Cistron A (*am*86)-[b]dependent
3	0.25–0.325	2 ± 2	~57,000	0.27 ± 0.03	Host
4	0.325–0.40	33 ± 2	50,000	0.37 ± 0.02	Cistron F (*am*87)
5	0.40–0.45	1 ± 1			None[c]
6	0.45–0.575	7 ± 3	37,000	0.50 ± 0.02	67% Cistron H (*am*N1)
			34,000	0.52 ± 0.02	33% Cistron C (*och*6) or I(?)
7	0.575–0.675	16 ± 2	25,000	0.59 ± 0.02	10% Cistron B (*am*16)
			20,500	0.63 ± 0.02	70% Cistron G (*am*9)
8	0.675–0.775	21 ± 3	17,500	0.68 ± 0.02	15% Cistron E(?) (*am*27)[d]
			14,500	0.73 ± 0.03	70% Cistron D (*am*42)
			13,500	0.75 ± 0.02	15% Cistron A (*am*86)
9	0.775–0.875	10.5 ± 2	~9,000	0.82 ± 0.02	80% Cistron J(?) (*am*6)
			~7,000	0.84 ± 0.02	20% Cistron C (*och*6) or I(?)
10	0.875–1.00	0.5 ± 3			Fragment region

[a] Standard deviations are the result of averaging five *wt* gel patterns from the same preparation run on different days.

[b] The high molecular weight of this protein suggests that it may not be coded for by only cistron A. It may represent (in roughly decreasing order of probability) a readthrough to cistrons B and C, a cistron A-induced host protein, a covalently linked subunit structure, or a ϕX174 protein covalently linked to a preexisting host protein.

[c] A very faint cistron E-induced band is visible in this region on occasion.

[d] The $RF_{15\%}$ = 0.68 protein also contains ~20% of the region 7 counts.

mapping between cistrons E and F, is described below. On the basis of complementation tests, Tessman (15) suggested previously that translation proceeds from cistron G to cistron H for the closely related bacteriophage S13.

In Fig. 3 we have redrawn the φX174 genetic map of nonsense mutations (1) as a hypothetical polycistronic message translated in the suggested direction and including the data of Tables 2 and 3. This is a reasonable assumption since Hayashi (8, 9) and Sedat (13) report that φX174 messenger ribonucleic acid (mRNA) is transcribed entirely from the complementary strand of replicative form DNA as one (or more) polycistronic message (messages). From this figure we may predict the effect of each nonsense mutation on the protein specified by the cistron containing it.

Major proteins. Mutants *op*6 (F), *am*9 (G), *am*42 (D), and several others are expected to eliminate the protein specified by their cistron. *am*27 (E), *am*88 (F), and *am*N1 (H) are expected to make fragments of altered mobility. *am*32 (G), *am*89 (F), and other mutations near the distal end of each cistron are predicted to have little detectable effect on the gel electrophoresis pattern. In the following sections, we test these predictions for each cistron.

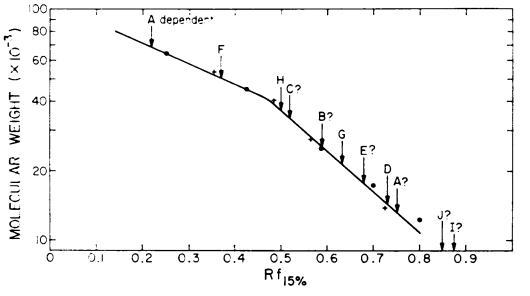

FIG. 2. *Molecular weights of φX174-specific proteins determined in 15% polyacrylamide SDS gels relative to proteins of known molecular weight. Albumin, ovalbumin, chymotrypsinogen, myoglobin, and cytochrome c were used as standards (●). In addition, ³H-labeled ribonuclease monomers, dimers, trimers, and tetramers (+) linked by diethyl pyrocarbonate (18) were used as internal standards to determine the molecular weight of ¹⁴C-labeled φX174 proteins. The molecular weights of the RF15% 0.82 and 0.84 proteins were determined on similar 20% polyacrylamide SDS gels (data not shown).*

(iv) Cistron D. Extracts of lysates of *am*42 (D), *am*10 (D), and *am*H81 (D)-infected nonpermissive cells do not show the $RF_{15\%}$ = 0.73 protein after electrophoresis on 15% polyacrylamide gels (Fig. 4). All other φX174-specific proteins appear to be present, and no fragments are detected. However, *am*10 (or *am*42, *am*H81)-infected cells make less of the proteins coded for by cistrons E, J?, F, G, and H than do *wt*-infected cells. This was determined by a ratio experiment in which ³H-labeled lysates from *wt*-infected cells were mixed with ¹⁴C-labeled lysates from *am*10 (D) mutant-infected cells (*data not shown*).

We interpret these results to mean that cistron D is the structural gene for the $RF_{15\%}$ = 0.73 protein, that our nonsense mutations lie near the N-terminal coding end of this cistron (i.e., no detected fragments), and that these nonsense mutations are weakly polar for distal cistrons translated in order D-E-F-G-H. The small genetic size of cistron D and the low molecular weight of this protein (14,500) are consistent with this evaluation.

After elimination of the cistron D protein, a small but distinct peak with $RF_{15\%}$ = 0.75 (we refer to the 0.74 peak in Fig. 4 as the $RF_{15\%}$ = 0.75 peak to correspond with the average value given in Table 1) can be observed (Fig. 4).

(v) Cistron E. Extracts of lysates of *am*3 (cistron E; Fig. 5b)- and *am*27 (cistron E; Fig. 5c)-infected nonpermissive cells show new polypeptide fragments on 20% gels. A 20% gel pattern of an extract of a lysate of *wt*-infected cells is shown in Fig. 5a for reference; 20% gels were used instead of 15% gels becase they allow greater separation of small-molecular-weight fragments. Both the *am*3 and *am*27 fragments are present in substantial quantity, suggesting that the cistron E product is made early and in large molar amounts. The *am*27

FIG. 3. *Genetic map of bacteriophage φX174 nonsense mutations redrawn as hypothetical polycistronic message. The order of cistrons is taken from Benbow et al. (1). The order of nonsense mutations within cistrons D, E, F, G, and H is taken from the data in Tables 2 and 3. amH81 (D) is not resolvable from am42 (D) by two-factor genetic crosses. The placement of och5 is based on the fact that it lies in complementation group B and maps less than 1 map unit from och6 in cistron C.*

TABLE 2. *Three-factor genetic crosses: order of am mutations within a cistron*

Cistron	Cross	Recombination frequency (× 10^4)	Percent	Predominant genotype	A	B	C	D	E	J(I)	F	G	H	A
D	(1) *am3ts9* × *am10*	1.5 ± 0.1	37	ts^a		9- - - - - - - - - - - -10- - - - - -3								
	(2) *am3ts9* × *am42*	2.0 ± 0.3	6	ts^a		9- - - - - - - -42- - - - - - - - - -3								
E	(3) *am3ts9* × *am27*	0.6 ± 0.2	22	*ts*		9- - - - - - - - - - - - -27- - - - -3								
	(4) *am3s*γ × *am27*	0.5 ± 0.2	88	*wt*				27- - - - -3- - - - - - - - - - - - -γ						
J(?)	(5) *am3ts9* × *am6*	0.1 ± 0.2	86	wt^b		9- - - - - - - - - - - - - - - - - - -3- - (6?)								
	(6) *am3ts*γ × *am6*	0.1 ± 0.2	41	ts^b						3- - (6?)- - - - - - - - -γ				
F	(7) *am88ts79* × *op9*	15.5 ± 4.2	99	*wt*						9- - - - -88- - - - -79				
	(8) *am88ts79* × *op6*	13.4 ± 3.7	91	*wt*						6- - - - -88- - - - -79				
	(9) *am88ts79* × *am*H57	1.4 ± 0.3	99	*wt*						H57- -88- - - - -79				
	(10) *am88ts79* × *am87*	0.3 ± 0.2	38	*ts*							88- -87- -79			
	(11) *am88ts79* × *am89*	0.5 ± 0.2	35	*ts*							88- -89- -79			
G	(12) *am9ts128* × *am32*	1.3 ± 0.4	33	*ts*								9- - -32- - - - - - 128		
H	(13) *am*N1*ts*γ × *am23*	0.3 ± 0.2	43	*ts*								γ- - -23-N1		
	(14) *am*N1*ts*γ × *am80*	0.4 ± 0.7	84	*wt*								γ- - - - -N1-80		
	(15) *am23ts4* × *am*N1	0.2 ± 0.3	10	*ts*								23-N1- - -4		
	(16) *am*N1*ts*γ × *am90*	1.3 ± 0.5	37	*ts*								γ- - -90-N1		

[a] The percentage of *ts* segregants in cross 2 is much higher (94%) than in cross 1 (63%), strongly suggesting that *am*42 is more closely linked than *am*10 to *ts*9.

[b] The recombination frequency in crosses 5 and 6 is sufficiently low that these results are based on plaque counts that were only three times the spontaneous reversion level.

TABLE 3. *Cistron F two-factor recombination frequencies (×10⁻⁴/total progeny phage)*

Mutant	Recombination values			
	*am*H57	*am*88	*am*87	*am*89
*am*H57	0.1			
*am*88	0.7 ± 0.3	0.05		
*am*87	0.9 ± 0.3	0.3 ± 0.4	0.05	
*am*89	1.5 ± 0.4	1.0 ± 0.4	0.45 + 0.4	0.03

fragment is of greater mobility, as predicted by its position nearer to the N-terminal end of the cistron. Both fragments are found in a region which contains no φX174 proteins in *wt* gel patterns. These data independently establish the direction of translation for cistron E from *am*27 to *am*3, corresponding to cistron order D-E-F-G-H-ABC.

An autoradiograph of a 15% polyacrylamide SDS gel of a lysate of *am*27 (E)-infected cells is shown in Fig. 6a. The $RF_{15\%}$ = 0.68 protein is present in reduced amounts, if at all. A similar pattern was obtained for *am*3 (E). It is thus likely that cistron E codes for the $RF_{15\%}$ = 0.68 protein of 17,500 molecular weight. However, in view of polar effects and the difficulties involved in detecting this protein, this identification is tentative.

(vi) Cistron J(?). Identification of the cistron E protein also is complicated by the behavior of *am*6 (J?), a nonsense mutant originally assigned to cistron E. Mutants in cistron E are unable to lyse nonpermissive host cells; *am*6 (J?) similarly fails to cause lysis of nonpermissive host cells. However, it clearly differs from our other cistron E mutants [*am*3 (E), *am*20 (E), *am*24 (E), *am*26 (E), *am*27 (E), *am*29 (E), and *am*34 (E)] in several respects.

(i) An autoradiograph of a lysate of *am*6 (J?)-infected cells (Fig. 6b) suggests that the $RF_{15\%}$ = 0.68 protein is present in *increased* amounts, as is the cistron D protein ($RF_{15\%}$ = 0.73). Furthermore, unlike the case for *am*3 (E) and *am*27 (E), extracts of lysates of *am*6 (J?)-infected cells are clearly missing the $RF_{15\%}$ = 0.82 protein as shown in Fig. 6c (compare Fig. 1b). φX174 deletion mutants shown to lack most of cistron E (A. J. Fuccarelli et al., Proc. Nat. Acad. Sci. U.S.A., *in press*) make the $RF_{15\%}$ = 0.82 protein in nearly normal amounts.

(ii) Nonpermissive cells infected with *am*6 (J?) do not produce infective intracellular particles. Instead, they accumulate defective particles which were examined on 15% gels (Fig. 7b). For comparison, *am*27 (E) virions (Fig. 7a) grown in the same nonpermissive host have five structural components (Table 4) of the same mobility as

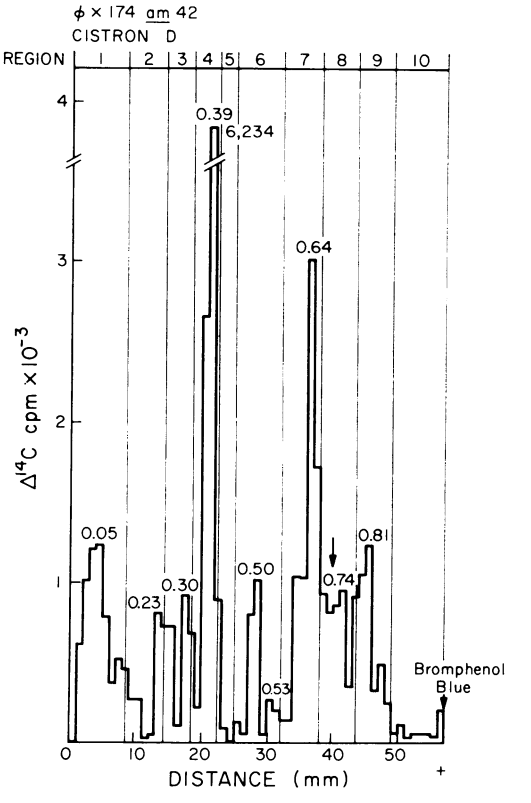

FIG. 4. *A 15% polyacrylamide SDS gel electrophoresis pattern of an extract of a lysate of* ^{14}C*-labeled am42 (D)-infected cells mixed with an extract of a lysate of* ^{3}H*-labeled uninfected cells. A peak with average mobility* $RF_{15\%}$ = 0.75 *(range = 0.74 to 0.76) is visible after elimination of the cistron D protein; the unusually wide band at* $RF_{15\%}$ = 0.73 *visible in autoradiographs of wt-infected cells (Fig. 1a) is consistent with the idea that the* $RF_{15\%}$ = 0.75 *peak represents another protein and not residual cistron D protein.*

those seen in *wt* virions (2, 3, 7), suggesting that cistron E does not specify a phage structural component. The ratio of ^{14}C-*wt*: ^{3}H-*am*6 (J?) or ^{14}C-*wt*: ^{3}H-*am*27 (E) virions coelectrophoresed in 15% gels is shown in Fig. 7c. The *am*6 (J?)-defective particles apparently are missing some capsid protein and most of the small structural component ($RF_{15\%}$ = 0.82).

These data imply either that *am*6 is in a separate cistron (J?) which complements poorly with cistron E, or that *am*6 does lie in cistron E, but in some manner interferes with the assembly of φX174 particles, whereas other cistron E mutants do not. The behavior of *am*6 in mapping experiments is consistent with the first idea. Unlike *am*27 (E), *am*6 (J?) cannot be resolved from *am*3 (E) during three-factor crosses. Two-factor recombination frequencies suggest the order *am*10

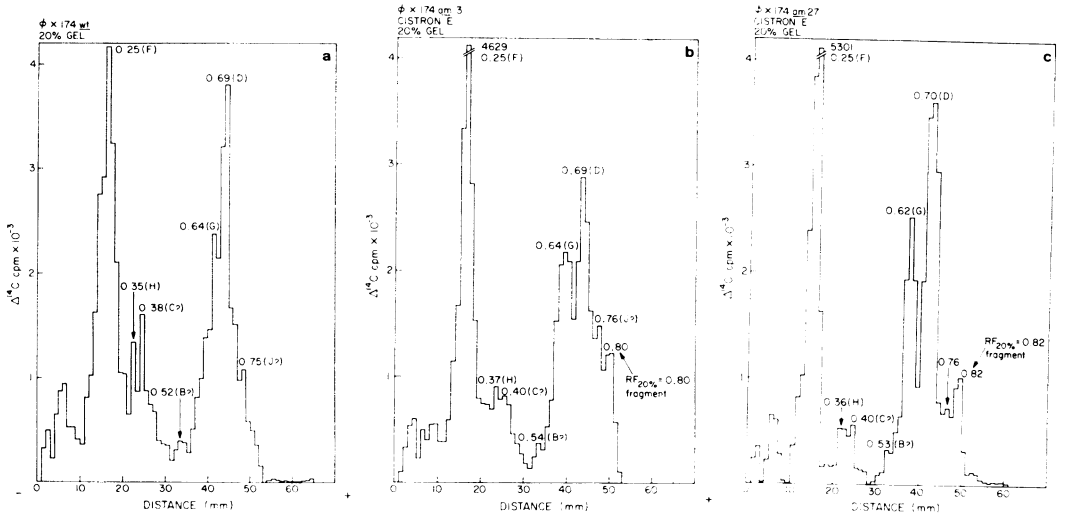

FIG. 5. *(a) A 20% polyacrylamide SDS gel electrophoresis pattern of an extract of a lysate of ^{14}C-labeled wt-infected cells mixed with an extract of a lysate of ^{3}H-labeled uninfected cells. In this gel, no φX174-specific proteins of mobility greater than $RF_{20\%}$ = 0.75 are seen. (b) A 20% polyacrylamide SDS gel electrophoresis pattern of an extract of a lysate of ^{14}C-labeled am3 (E)-infected cells mixed with an extract of a lysate of ^{3}H-labeled uninfected cells. (c) A 20% polyacrylamide SDS gel electrophoresis pattern of an extract of a lysate of ^{14}C-labeled am27 (E)-infected cells mixed with an extract of a lysate of ^{3}H-labeled uninfected cells.*

(D)-*am*27 (E)-*am*3 (E)-*am*6 (J?)-*op*6 (F) (*unpublished data*). Perhaps the simplest solution is that *am*6 lies at the N-terminal end of a new cistron J, which codes for the smallest structural component of the virion, and that this cistron product must be present in large amounts to interact with the cistron E protein for normal lysis to occur.

(vii) Cistron F. Cistron F codes for the φX174 capsid protein (4, 11) of 50,000 molecular weight (3, 6). Nonsense mutations in this cistron have been mapped at loci covering over 20% of the φX174 genome. Our predictions regarding the effect of the position of a nonsense mutation relative to the N-terminal coding end of the cistron are strikingly supported: *am*87 (F), near the distal end of the cistron, codes for a capsid fragment of about 43,000 molecular weight (Fig. 8a). *op*6 (F) (Fig. 8b), at the proximal end of the cistron, eliminates the capsid protein from extracts of lysates of infected cells and, in addition, strongly diminishes the amount of G and H proteins made (*see below*). During *op*6 (F) infection the proteins specified by cistrons D, E, and J(?) are made in somewhat greater than normal amounts as determined by a ratio experiment. These data are consistent with the interpretation that *op*6 (F) is a strong polar mutation in a polycistronic message that starts with cistron D and contains D, E, J(?), F, G, and H. Cistrons A, B, and C might either be on the same mRNA with a separate initiator site or on a different mRNA entirely. Complementation tests (Table 5) support these conclusions in that *op*6 (F) does not complement cistron F mutants, complements poorly with cistron G and H mutants, yet complements reasonably well with cistron B mutants.

Several controls were done to insure that the *op*6 (F) mutation is not unique for unrelated reasons. A second opal mutant, *op*9 (F), was isolated near to the *op*6 (F) locus. Extracts of lysates of cells infected with *op*9 (F) show a similar gel pattern (*not shown*) to that of *op*6 (F). *op*9 (F), however, has different plaque morphology and is resolvable from *op*6 (F) by two-factor genetic crosses. These opal mutants are definitely single-base transition mutants as shown by reversion frequencies (to *wt*) of approximately 10^{-6}. Extracts of lysates of cells infected with opal mutants in other cistrons show less drastically altered gel patterns. I. Tessman has pointed out that we are unable to exclude rigorously the possibility that *op*6 (F) lies not in cistron F, but in a special initiator region for cistrons F, G, and H. He also reports the existence of a similar *op* mutation in (or near) S13 cistron F (*personal communication*). We believe that the simplest interpretation is that these opal mutants are strong polar mutations near the N-terminal coding end of cistron F.

The direction of translation from cistron D through E, F, G, and H is supported by the size

of fragments generated by a linear series of nonsense mutations within cistron F (11). To show this, we have taken advantage of the fact that the capsid protein (F) is directly visible as a large radioactive peak in 10% gel patterns of extracts of lysates of labeled φX174-infected cells. ^{3}H-labeled virions containing over 70% *wt* capsid protein on a counts per minute basis were denatured and run in the same gel as ^{14}C-labeled extracts of lysates of nonpermissive cells infected with a mutant in cistron F. In Fig. 9 shifts to smaller molecular weight (47,000) are evident in the mobility of *am*89 (F) and *am*88 (F) capsid fragments relative to *wt* capsids. *am*87 (F) and *am*H57 (F) show similar shifts to 43,000 and 40,500 molecular weight, respectively. The size of each capsid fragment is proportional to the distance of the mutation from the N-terminal coding end of cistron F. These shifts in mobility independently support the direction of translation D-E-F-G-H-A-B-C.

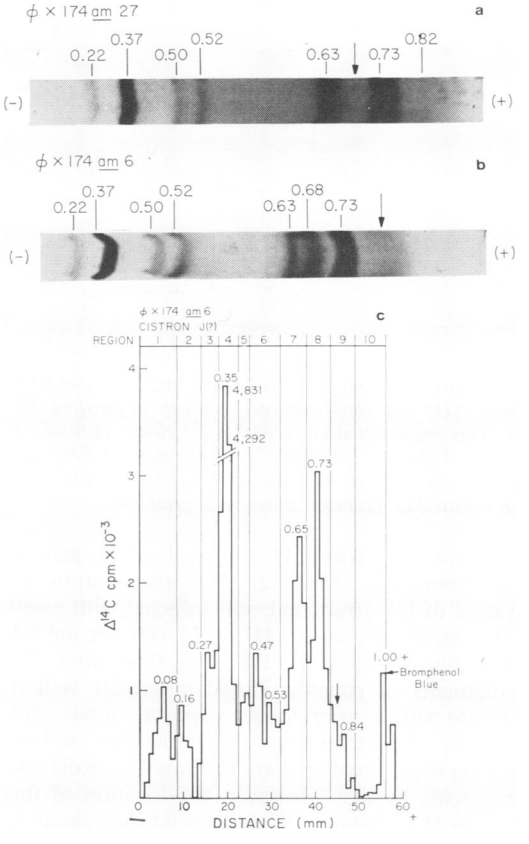

FIG. 6. (*a*) *An autoradiograph of a 15% polyacrylamide SDS gel of a lysate of* ^{14}*C-labeled am27 (E)-infected, UV-irradiated cells. The* $RF_{15\%}$ *= 0.68 protein is present in reduced amounts, if at all. An am3 (E) infection (not shown) results in a similar autoradiograph. An infection with am34 (E) (also not shown), which maps at the extreme distal end of cistron E, results in autoradiographs missing a band at* $RF_{15\%}$ *= 0.68, but possessing a new band at* $RF_{15\%}$ *= 0.70, i.e., closer to the cistron D (*$RF_{15\%}$ *= 0.73) band. (b) An autoradiograph of a 15% polyacrylamide SDS gel of a lysate of* ^{14}*C-labeled am6 (J?)-infected, UV-irradiated cells. The* $RF_{15\%}$ *= 0.68 protein is present in increased amounts relative to the bands seen in wt infections (Fig. 1a). The* $RF_{15\%}$ *= 0.82 protein is missing (see part c) though a faint band from the* $RF_{15\%}$ *= 0.84 protein is still visible. (c) A 15% polyacrylamide SDS gel electrophoresis pattern of an extract of a lysate of* ^{14}*C-labeled am6 (J?)-infected cells mixed with an extract of a lysate of* ^{3}*H-labeled uninfected cells. The* $RF_{15\%}$ *= 0.82 peak is missing, and a fragment migrating with the bromphenol blue dye marker is seen. A small peak of* $RF_{15\%}$ *= 0.84 is now visible.*

(viii) Cistron G. An extract of a lysate of *am*9 (G)-infected cells is shown in Fig. 10. The gel pattern is missing a peak with $RF_{15\%}$ = 0.63 and has a strongly diminished peak of $RF_{15\%}$ = 0.50. A similar effect was seen by Gelfand and Hayashi (6) for *am*H116 (G). We have been unable to isolate mutants in cistron G that generate fragments with visibly altered mobilities. *am*32 (G) apparently codes for a (nearly) normal protein (gel pattern not shown) as expected from its position on the genetic map. From the map position of *am*9 at the N-terminal coding end of cistron G, it is reasonable to suggest that the $RF_{15\%}$ = 0.63 protein is coded for by cistron G and that *am*9 is polar for the $RF_{15\%}$ = 0.50 protein (shown below to be coded for by cistron H).

Another line of evidence suggests that cistron G is the structural gene for the $RF_{15\%}$ = 0.63 protein. *wt* virions and 70*S* particles contain a protein which coelectrophoreses on SDS polyacrylamide gels with the $RF_{15\%}$ = 0.63 protein (2, 11, S. Krane, Ph.D. thesis, California Inst. of Technology, Pasadena, 1968). Bacteriophage particles of the *ts*79 mutant (a temperature-sensitive mutation in cistron G), prepared at 30 C, contain this same component in SDS gels, but it exhibits an altered electrophoretic mobility in *urea* gels (4). Therefore, the *ts*79 (G) mutation is in the $RF_{15\%}$ = 0.63 protein.

Complementation tests (Table 5) also support the conclusion that *am*9 (G) is a strong polar mutation since *am*9 (G) complements poorly with cistron H mutants, whereas *ts* mutants in cistron G show adequate complementation with cistron H mutants (9, 15).

As shown in Fig. 10, two additional φX174-specific proteins are visible when the $RF_{15\%}$ = 0.63 protein is eliminated. The $RF_{15\%}$ = 0.68 protein typically is visible in autoradiographs (see

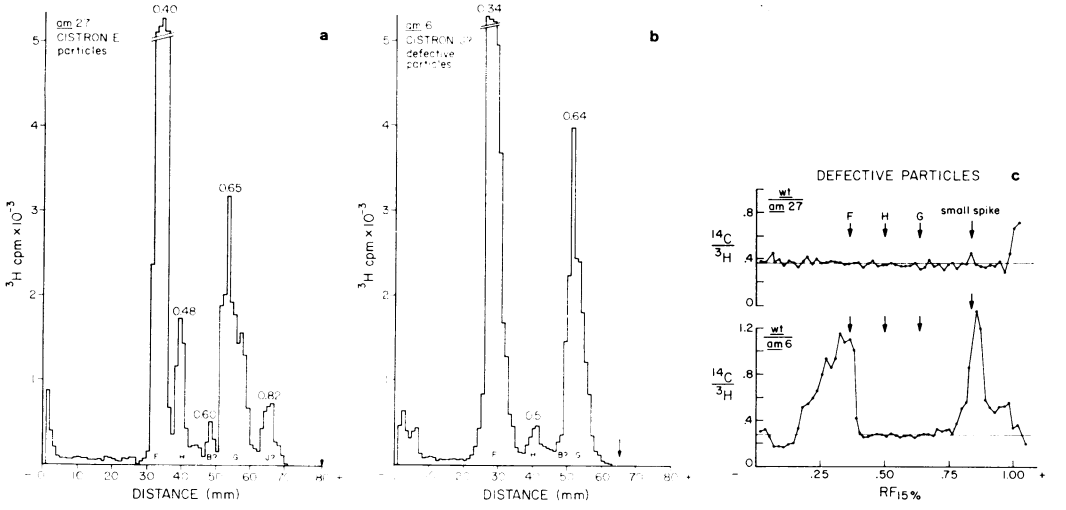

FIG. 7. *(a) A 15% polyacrylamide SDS gel electrophoresis pattern of purified ^{3}H-labeled am27 (E) particles prepared in a nonpermissive host. (b) A 15% polyacrylamide SDS gel electrophoresis pattern of purified ^{3}H-labeled am6 (J?) particles prepared in a nonpermissive host. This preparation is exceptionally clean; typically 1 to 2% of the total counts are seen in the small spike region (see Table 4). (c) A 15% polyacrylamide SDS gel electrophoresis pattern of the ratio of ^{14}C-labeled wt:^{3}H-labeled am6 (J?) or ^{14}C-labeled wt:^{3}H-labeled am3 (E) virions run in the same gel. Purification by CsCl banding was omitted to minimize selective degradation.*

TABLE 4. *Percentage of composition of φX174 virions (^{3}H- or ^{14}C-leucine labeled)*

Virion	Percent composition				
	Cistron products				
	F	H	B?	G[a]	J?
*am*3[b] (E)	66.7	7.6	—	20.2	5.5
wt[c]	64.5	4.0	3.9	24.8	2.8
*am*27 (E)	64.5	6.6	1.4	22.9	3.7
*am*6 (J?)	64.5	4.1	1.1	29.0	*1.3*
*am*N1 (H)	75.6	*0.4*	1.1	19.3	3.6

[a] A variable percentage of the cistron G counts are seen as a leading edge which we believe to represent a contaminant, but which may represent a sixth component of the φX174 virion (A. J. Zuccarelli, R. M. Benbow, and R. L. Sinsheimer, Proc. Nat. Acad. Sci. U.S.A., *in press*).

[b] Uniformly amino acid labeled, taken from Burgess (2).

[c] Taken from A. J. Zuccarelli, R. M. Benbow, and R. L. Sinsheimer, Proc. Nat. Acad. Sci. U.S.A., *in press*.

Fig. 1a) and is diminished by the *am*27 (E) mutation. The $RF_{15\%}$ = 0.59 protein is visible only when the $RF_{15\%}$ = 0.63 protein is absent. We believe the $RF_{15\%}$ = 0.59 protein is a minor component of the φX174 virion (Fig. 7b) and is coded by cistron B (*see below*).

(ix) Cistron H. Several independent nonsense mutations in cistron H are resolved by genetic recombination (Table 2). Autoradiographs of lysates of UV-irradiated cells infected with *am*80 (H), *am*90 (H), *am*23 (H), *op*11 (H), or *am* N1 (H) (Fig. 11) lack the $RF_{15\%}$ = 0.50 band (7). Fragments of roughly 25,000 molecular weight (7) are visible after longer exposure times (*not shown*); the differences in molecular weight among these fragments are too small to order the fragments by size. However, the location of the cistron H mutations on the genetic map predicts a series of fragments in this molecular weight range if cistron H is translated in the direction G→ H-A-B-C.

Minor proteins. None of the remaining four (or five) φX174-specific proteins—which are made in relatively small molar amounts—can be firmly assigned to cistrons.

(x) Cistron A. We confirm the report of Godson (7) that mutants in cistron A eliminate the $RF_{15\%}$ = 0.22 protein. However, we also observe the disappearance of the $RF_{15\%}$ = 0.75 protein (Fig. 12). In view of the high molecular weight of the $RF_{15\%}$ = 0.22 protein, we prefer to assign cistron A as the structural gene for the $RF_{15\%}$ = 0.75 protein.

Regardless of whether we correctly identify the remaining φX174 cistrons, our data support the direction of translation ABC. Mutants *am*50 (A) and *am*86 (A) decrease the amounts of $RF_{15\%}$ = 0.84, 0.52, and 0.59 proteins (*data not shown*), suggesting they are weak polar mutations as predicted

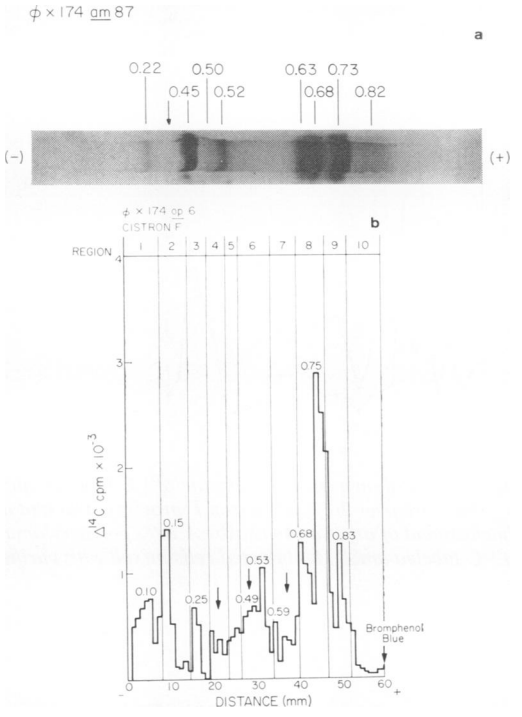

FIG. 8. *(a) An autoradiograph of a 15% polyacrylamide SDS gel of a lysate of ^{14}C-labeled am87 (F)-infected, UV-irradiated cells. Arrow points to the normal ($RF_{15\%}$ = 0.37) position of the cistron F protein. A new $RF_{15\%}$ = 0.45 band is present. am87 (F) is weakly polar based on the fact that possibly the cistron G ($RF_{15\%}$ = 0.63) and certainly the H ($RF_{15\%}$ = 0.50) band are more faint than in wt-infected cells. (b) A 15% polyacrylamide SDS gel electrophoresis pattern of an extract of a lysate of ^{14}C-labeled op6 (F)-infected cells mixed with an extract of a lysate of ^{3}H-labeled uninfected cells. This strong polar mutant eliminates or reduces three separate peaks (indicated by arrows). Protein peaks with $RF_{15\%}$ = 0.68 and $RF_{15\%}$ = 0.59 are now visible.*

by their position on the genetic map. In addition, *am*35 (A) and *am*18 (A) fail to complement well with cistron B mutants (10) although little decrease in the $RF_{15\%}$ = 0.82 and $RF_{15\%}$ = 0.59 proteins is detected.

(xi) Cistron B. None of our mutations in cistron B eliminate any major proteins from 15% gel patterns. We assign the $RF_{15\%}$ = 0.59 (molecular weight = 25,000) protein to cistron B for the following reasons: (i) *am*16 (B) eliminates the $RF_{20\%}$ = 0.52 protein in 20% gels when examined by a double-label procedure (Fig. 13). This protein corresponds to the $RF_{15\%}$ = 0.59 protein (which typically is obscured on 15% gels, but see Fig. 10). (ii) Virions of several cistron B mutants (*am*14 [B], *am*16 [B], *ts*9 [B]), grown in permissive host cells show an altered thermal

TABLE 5. *Complementation of strong polar mutants (normal wt burst size of 100)*

Mutants	Burst size	Complementation
*op*6 (F)		
*op*6 (F) × *am*16 (B)	14.8	+
*op*6 (F) × *ts*4 (H)	2.4	−
*op*6 (F) × *am*9 (G)	2.4	−
*op*6 (F) × *am*88 (F)	0.8	−
*am*9 (G)		
*ts*79 (G) × *am*23 (H)	33.6	+
*ts*4 (H) × *am*23 (H)	3	−
*am*9 (G) × *am*23 (H)	3	−

stability (10); since one or two $RF_{15\%}$ = 0.59 proteins are seen per virion (Fig. 7b, see also Godson [7]), the altered thermal stability may be due to alterations in the cistron B protein structure.

The direction of translation of cistron B is established by the fact that *am*16 (B) at the proximal end of cistron B causes, presumably by a polar effect, a decrease in the $RF_{15\%}$ = 0.84 and $RF_{20\%}$ = 0.52 proteins, whereas *och*5 (B) at the distal end of cistron B does not. This is most clearly seen on 12% gels (*data not shown*).

(xii) Cistron C (and I?). Extracts of lysates of *och*6 (C)-infected cells are missing the $RF_{20\%}$ = 0.40 peak on 20% gels (Fig. 14). This probably corresponds to the $RF_{15\%}$ = 0.52 protein of 34,000 molecular weight. In addition, the $RF_{15\%}$ = 0.84 protein is diminished on 15% gels (*not shown*). A new fragment is observed of $RF_{20\%}$ = 0.80 (~6,000 molecular weight) which is consistent with the proposed map position of *och*6 (C). This confirms the earlier report of a cistron C fragment by Tessman for the related bacteriophage S13 (Virology, 1971, *in press*). We are unable to establish whether cistron C is the structural gene for the $RF_{15\%}$ = 0.52 or 0.84 proteins. Cistron I presumably codes for the other of these two proteins. Cistron C protein is required only in very small amounts (5), consistent with the idea that it is nearly the last protein translated.

DISCUSSION

The purpose of this paper is twofold: to define the direction of translation of φX174 cistrons and to demonstrate the approximate proportionality of the φX174 genetic map and the φX174 physical genome defined by protein molecular weights. These conclusions do not depend on the correct identification of every cistron product, although the agreement of much of our data with that of

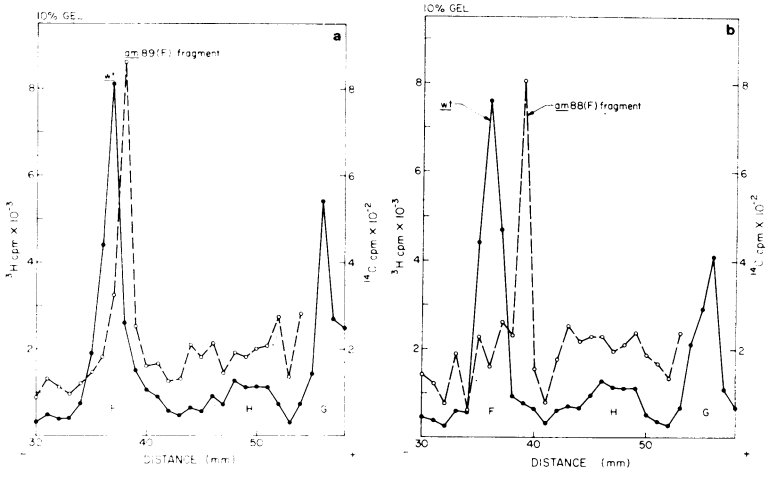

FIG. 9. *(a) A 10% polyacrylamide SDS gel electrophoresis pattern of an extract of a lysate of ^{14}C-labeled am89 (F)-infected cells mixed with purified ^{3}H-labeled wt virions (which are over 70% wt cistron F protein). The mutant capsid fragment is visible as a distinct peak well above the background of other proteins. (b) A 10% polyacrylamide SDS gel electrophoresis pattern of an extract of a lysate of ^{14}C-labeled am88 (F)-infected cells mixed with purified H-labeled wt virions.*

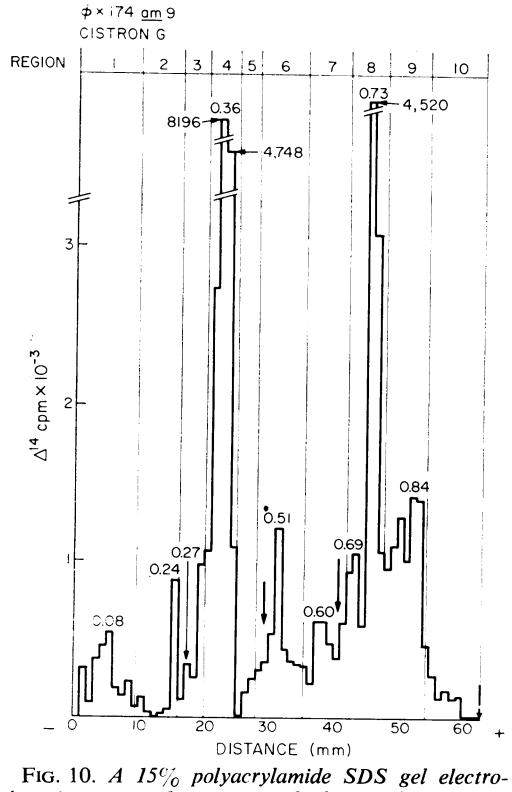

FIG. 10. *A 15% polyacrylamide SDS gel electrophoresis pattern of an extract of a lysate of ^{14}C-labeled am9 (G)-infected cells mixed with an extract of a lysate of ^{3}H-labeled uninfected cells. The $RF_{15\%}$ = 0.59 and $RF_{15\%}$ = 0.68 proteins are again visible.*

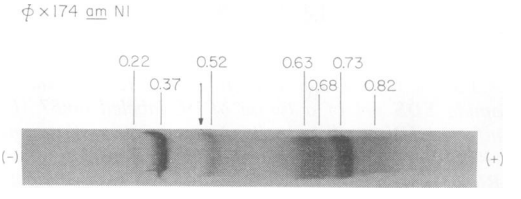

FIG. 11. *An autoradiograph of a 15% polyacrylamide SDS gel of a lysate of ^{14}C-labeled amN1 (H)-infected UV-irradiated cells. Measurements on numerous independent gels of cistron H mutants establish unambiguously that the $RF_{15\%}$ = 0.50 protein (and not the 0.52 protein) is eliminated by cistron H mutations.*

other groups (2, 3, 6, 7, 11) suggests that our attributions are substantially correct.

Direction of translation of the φX174 genome. Direction of translation of the φX174 genome proceeds in cistron order D-E-F-G-H-A-B-C. The order of translation G → H was first suggested by Tessman for the related bacteriophage S13 on the basis of complementation tests (15). This has since been confirmed several times, most recently by experiments using mutants in cistron F similar to those described above (17). In this paper we establish that bacteriophage φX174 is translated in the same direction as bacteriophage S13, and not the reverse as reported by Hutchison (C. A. Hutchison III, Ph.D. thesis, California Inst. of Technology, Pasadena, 1969). Several independent lines of evidence establish this direction.

(i) Nonsense mutations at the proximal end of

each cistron (read in the direction D-E-F-G-H-A-B-C) such as *am*42 (D), *op*6 (F) and *am*9 (G) eliminate one (or more) φX proteins from gel patterns of extracts of lysates of infected cells,

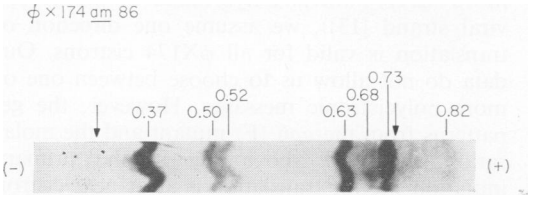

FIG. 12. *An autoradiograph of a 15% polyacrylamide SDS gel of a lysate of* ^{14}*C-labeled am86 (A)-infected UV-irradiated cells. As reported earlier by Godson (7), the* $RF_{15\%}$ *= 0.22 band is absent; in addition, the cistron D band (*$RF_{15\%}$ *= 0.73) is sharpened and narrower than in wt-infected cells. We interpret this to mean that the* $RF_{15\%}$ *= 0.75 protein shown in Fig. 4 also is eliminated by the am86 (A) mutation. A similar gel was sectioned into 0.5-mm slices with a Mickel gel slicer, and the percentage of total counts in each region was calculated relative to the gel pattern for wt-infected UV-irradiated cells. Decreases were found in the* $RF_{15\%}$ *= 0.22 and 0.74 regions.*

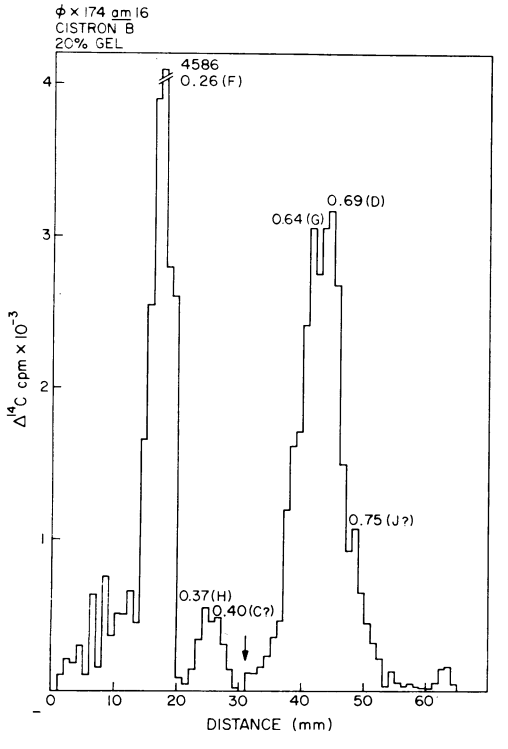

FIG. 13. *A 20% polyacrylamide SDS gel electrophoresis pattern of an extract of a lysate of* ^{14}*C-labeled am16 (B)-infected cells mixed with an extract of a lysate of* ^{3}*H-labeled uninfected cells. For comparison, a wt pattern on a 20% gel is found in Fig. 5a.*

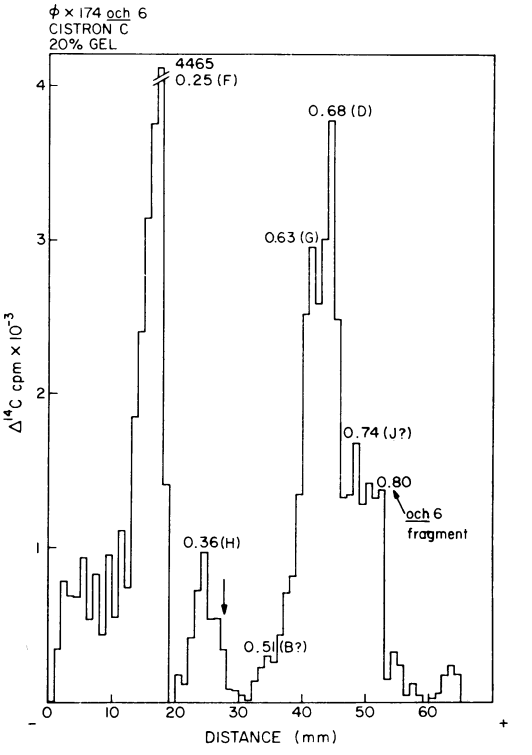

FIG. 14. *A 20% polyacrylamide SDS gel electrophoresis pattern of an extract of a lysate of* ^{14}*C-labeled och6 (C)-infected cells mixed with an extract of a lysate of* ^{3}*H-labeled uninfected cells. For comparison, a wt pattern on a 20% gel is found in Fig. 5a.*

whereas those near the distal ends such as *am*89 (F) and *am*32 (G) have little detectable effect on the mobility of single proteins.

(ii) In cistrons E and F, where a series of internal nonsense mutations are ordered by three-factor crosses (*am*27 [E]-*am*3 [E]) and (*am*H57 [F]-*am*88 [F]-*am*89 [F]), shifts in the mobilities of polypeptide fragments are consistent with the order D-E-F-G-H-A-B-C deduced above. In addition, the fragments found with cistron H mutants support this direction of translation.

(iii) The gel patterns of several strong polar mutations—*op*6 (F) and *op*9 (F) in cistron F (eliminating G and H) and *am*9 (G) in cistron G (eliminating H)—support this direction of translation. Weak polar effects consistent with this direction are observed for other mutations, such as *am*10 in cistron D and *am*86 in cistron A. Our data also suggest that cistrons in front of a polar mutation are translated in greater molar amounts.

(iv) Complementation tests of these strong polar mutants (*op*6 [F] and *am*9 [F], see Table 4) confirm their pleiotropic effects in nonpermissive cells. In addition, the mutants *am*35 (A) and

*am*18 (A) (both in the high recombination region of cistron A) fail to complement the adjacent cistron B. This again suggests the direction A → B-C-D-E-F-G-H. Mutants *am*35 (A) and *am*18 (A) originally were mapped in cistron B (C. A. Hutchison III, Ph.D. thesis, California Inst. of Technology, Pasadena, 1969) accounting for the suggestion by Hutchison of the reverse order (B → A) of translation.

(v) The in vivo molar proportions of uniformly labeled (by ^{14}C-amino acid mixture) ϕX174 proteins progressively decrease starting at cistron D. The molar ratios, normalized to 1.0 mole of cistron F product (chosen because it is the most thoroughly characterized protein at present), are 2.0 (D):1.2 (J?):1.0 (F):0.94 (G):0.2 (H):0.2 (A): ~0.1 (B): ~0.1 (C). Little change in these molar ratios is seen if Δ^{14}C-leucine counts are used, but gross variations occur if Δ^{14}C-arginine or -lysine counts are employed.

Since ϕX174 mRNA is transcribed entirely from the complementary strand (less than 1 part in 10^6 ϕX174 mRNA hybridizes to the ϕX174 viral strand [13]), we assume one direction of translation is valid for all ϕX174 cistrons. Our data do not allow us to choose between one or more polycistronic messages. However, the gel patterns from the *op*6 (F) mutant and the molar ratios calculated above suggest the primary initiation site for translation is at or near cistron D, and that cistrons A, B, and C have a separate (or at least independent) initiation site from the D-E-F-G-H operon.

Cistrons of like function such as the major virus coat cistrons appear to be clustered on the genome and under coordinated control. Also,

TABLE 6. *Proportionality of ϕX174 physical and genetic maps*

Determination	Genetic size[a]	Measured mol wt	wt Recombinants/nucleotide[b]
(I) Cistron sizes			
Cistron D	1.3×10^{-4}	14,500	3.7×10^{-7}
E	1.3×10^{-4}	17,500	3.1×10^{-7}
F	6.4×10^{-4}	50,000	5.3×10^{-7}
G	2.0×10^{-4}	20,500	4.0×10^{-7}
H	3.3×10^{-4}	37,000	3.7×10^{-7}
A	~2.0×10^{-4}[c]	14,000 (or 67,000)	5.92×10^{-7} (1.2×10^{-7})
B	2.2×10^{-4}	25,000	3.6×10^{-7}
C	1.5×10^{-4}	34,000 (or 7,000)	1.8×10^{-7} (8.9×10^{-7})
J(?)	~1.0×10^{-4}	9,000	4.6×10^{-7}
I(?)	?	7,000 or 34,000	?
All cistrons	24.4×10^{-4}	228,000	4.4×10^{-7}
A "hairpin"	30.0×10^{-4}[d]	14,000 (or 67,000)	88.9×10^{-7} (18.5×10^{-7})
(II) Distances between intracistronic markers			
*am*88 (F)-*am*89 (F)	1.0×10^{-4}	5,700	7.3×10^{-7}
*am*3 (E)-*am*27 (E)	0.6×10^{-4}	3,000	8.3×10^{-7}
*am*H57 (F)x *am*89 (F)	1.5×10^{-4}	7,200	8.6×10^{-7}
(III) Distances between intercistronic markers			
*am*10-*am*9	9.0×10^{-4}[a]	~88,500	4.2×10^{-7}
*am*9-*am*86	5.0×10^{-4}[a]	~59,500	3.5×10^{-7}
*am*N1-*am*16	7.7×10^{-4}[a]	~47,000 (or 100,000)	7.7×10^{-7} (3.6×10^{-7})
*am*16-*am*10	3.1×10^{-4}[a]	~67,000	1.9×10^{-7}
(IV) Apparent exceptions[e]			
*am*33 (A)-*am*18 (A)[f]	21.9×10^{-4}	~10,000 (or 63,000)	90.8×10^{-7} (14.4×10^{-7})
*am*86 (A)-*am*35 (A)[f]	16.8×10^{-4}	~14,000 (or 67,000)	49.7×10^{-7} (10.4×10^{-7})
*och*6 (C)-*am*9 (G)[f]	1.2×10^{-4}	~115,000	0.43×10^{-7}
*am*23 (H)-*am*3 (E)[f]	2.2×10^{-4}	~98,500	0.93×10^{-7}

[a] Genetic sizes were read directly off the map (reference 1, Fig. 1) except where indicated; this genetic size is often larger than the recombination frequency between the markers for the reasons noted in (1).

[b] Since 5,500 nucleotides code for 228,000 daltons protein molecular weight, the number of nucleotides covered by a protein can be estimated by dividing the protein molecular weight by 41.45.

[c] Estimated by the distance across cistron A (reference 1, Fig. 2), not the distance within it.

[d] Taken from genetic map in reference 1, Fig. 2.

[e] Cases where an individual marker gives an abnormally high or low recombination value—these may represent site-specific recombination effects as described in (1).

[f] Actual recombination frequency, not map distance.

och mutations are found only in cistrons B and C—presumably among the last cistrons to be translated.

Genetic map distances on bacteriophage φX174 genome. Genetic map distances on bacteriophage φX174 genome are approximately proportional to physical distances represented by φX174 protein molecular weights. This conclusion is used as a starting point for an analysis of the primary and secondary mechanisms of genetic recombination for bacteriophage φX174 DNA. It also serves as the foundation for the mapping by electron microscopy of structural features of the φX174 genome using the cistron E deletion (A. J. Zuccarelli, R. M. Benbow, and R. L. Sinsheimer, Proc. Nat. Acad. Sci. U.S.A., *in press*) as a physical marker. Exceptions to proportionality are found in the high recombination region of cistron A. In addition, site- or marker-specific recombination effects analogous to those described by Norkin (12) are found for *am*23 (H), *och*6 (C), and perhaps other mutations (1), but these do not contradict our general conclusions.

Data establishing proportionality of the physical and genetic maps are summarized in Table 6. Genetic distances were taken from Tables 2 and 3 of this paper and from Benbow et al. (1). Physical distances (the molecular weights of protein or polypeptide fragments) were estimated from the data presented in this paper, principally from Fig. 2. Errors due to incorrect protein attributions for cistrons A, B, and C will have an insignificant effect on our general conclusions.

Several points are emphasized by these calculations.

(i) In general the genetic map of bacteriophage φX174 as previously drawn (1) accurately reflects physical distances (Table 6, part I). The cistron C region was slightly underestimated in length because of the low recombination values of *och*6 (C). The cistron A region was overestimated because of the abnormally high recombination values of most cistron A mutants. A more accurate map will be presented at a later date (R. M. Benbow, A. J. Zuccarelli, G. Davis, and R. L. Sinsheimer, *in preparation*) in conjunction with the φX174 genetic map in a *rec* A host.

(ii) Intracistronic recombination frequencies (Table 6, part II) are higher than the genome average of 4.4×10^{-7} *wt* recombinants/nucleotide as predicted by the phenomenon of map contraction described earlier (1). Intercistronic map distances (Table 6, part III) are roughly constant around the entire map.

(iii) Apparent exceptions to proportionality (Table 6, part IV) represent individual marker effects (12) and not genuine exceptions to proportionality.

Therefore, these data establish the colinearity and approximate proportionality of the complete genetic and physical maps of bacteriophage φX174. It should be noted that proteins of less than 6,000 molecular weight will not be observed in our gel patterns. With this reservation, the results in this paper taken together with the genetic map of bacteriophage φX174 (1) suggest that the 10 proposed cistrons account for the entire (>95%) φX174 genome.

ACKNOWLEDGMENTS

We thank Paul Howard-Flanders for the initial idea to study the genetic recombination of bacteriophage φX174. The excellent technical assistance of Gloria Davis, Alma Shafer. David Holmes, and Jill Fabricant Hiatt is acknowledged.

A preliminary account of these results was given at the Bacteriophage Meetings, Cold Spring Harbor, 27–31 August 1970.

This research was carried out with the assistance of Public Health Service training grant GM-86 and research grant GM13554 from the National Institute of General Medical Sciences.

LITERATURE CITED

1. Benbow, R. M., C. A. Hutchison III, J. D. Fabricant and R. L. Sinsheimer. 1971. Genetic map of bacteriophage φX174. J. Virol. 7:549–558.
2. Burgess, A. B. 1969. Studies on the proteins of φX174. II. The protein composition of the φX coat. Proc. Nat. Acad. Sci. U.S.A. 64:613–617.
3. Burgess, A. B., and D. T. Denhardt. 1969. Studies on φX174 proteins. I. Phage-specific proteins synthesized after infection of Escherichia coli. J. Mol. Biol. 44:377–386.
4. Edgell, M., C. A. Hutchison, and R. L. Sinsheimer. 1969. The process of infection with bacteriophage φX174. XXVIII. Removal of the spike proteins from the phage capsid. J. Mol. Biol. 42:547–557.
5. Funk, F. and R. L. Sinsheimer. 1970. Process of infection with bacteriophage φX174. XXXV. Cistron VIII. J. Virol. 6:12–19.
6. Gelfand, D. H., and M. Hayashi. 1969. Electrophoretic characterization of φX174-specific proteins. J. Mol. Biol. 44: 501–516.
7. Godson, G. N. 1971. Characterization and synthesis of φX174 proteins in ultraviolet-irradiated and unirradiated cells. J. Mol. Biol. 57:541–553.
8. Hayashi, M., M. N. Hayashi, and S. Spiegelman. 1963. Restriction of *in vivo* genetic transcription to one of the complementary strands of DNA. Proc. Nat. Acad. Sci. U.S.A. 50:664.
9. Hayashi, Y., and M. Hayashi. 1970. Fractionation of φX174 specific messenger RNA. Cold Spring Harbor Symp. Quant. Biol. 35:171–177.
10. Lindqvist, B., and R. L. Sinsheimer. 1967. The process of infection with bacteriophage φX174. XIV. Studies on macromolecular synthesis during infection with a lysis defective mutant. J. Mol. Biol. 28:87–94.
11. Mayol, R. F., and R. L. Sinsheimer. 1970. Process of infection with bacteriophage φX174. XXXVI. Measurement of virus-specific proteins during a normal cycle of infection. J. Virol. 6:310–319.
12. Norkin, L. C. 1970. Marker-specific effects in genetic recombination. J. Mol. Biol. 51:633–655.
13. Sedat, J., A. Lyon, and R. L. Sinsheimer. 1969. Purification of *Escherichia coli* pulse-labeled RNA by benzoylated DEAE-cellulose chromatography. J. Mol. Biol. 44:415–432.
14. Shapiro, A. L., E. Viñuela, and J. V. Maizel. 1967. Molecular

weight estimation of polypeptide chains by electrophoresis in SDS-polyacrylamide gels. Biochem. Biophys. Res. Commun. **28**:815–820.

15. Tessman, I., S. Kumar, and E. S. Tessman. 1967. Direction of translation in bacteriophage S13. Science **158**:267–268.
16. Yanofsky, C., B. C. Carlton, J. R. Guest, D. R. Helinski, and U. Henning. 1964. On the colinearity of gene structure and protein structure. Proc. Nat. Acad. Sci. U.S.A. **51**:266–272.
17. Vanderbilt, A. S. M. T. Borrás, and E. S. Tessman. 1971. Direction of translation in phage S13 as determined from the sizes of polypeptide fragments of nonsense mutants. Virology **43**:352–355.
18. Wolf, B., P. M. Lausarot, J. A. Lesnaw, and M. E. Reichman. 1970. Preparation of polymeric protein markers and an investigation of their behavior in sodium dodecyl sulfate-polyacrylamide gel electrophoresis. Biochim. Biophys. Acta **200**:180–183.
19. Zipser, D. 1970. Polar mutations and operon function. Nature (London) **221**:21–25.